Suppl. Figure 1. Cells cultured in oxLDL take up Oil Red O in a time-dependent manner. Uptake of Oil Red O was performed as detailed in *Materials and Methods* and absorbance of samples was expressed as units per milligram of total cellular protein. *A*, Representative donor analysis. *B*, 3 independent experiments with each condition tested in triplicate.

Suppl. Figure 2. OxLDL, 9-HODE and 13-HODE induce CXCL16 up-regulation on monocyte-derived Mϕ. Representative donor analysis of CXCL16 surface expression. Mo were cultured for 6, 12 or 24 h without (*A*) or with the following stimuli: 50 μg/ml LDL (*B*), 50 μg/ml oxLDL (*C*), 10 μg/ml PGPC (*D*), 10 μg/ml POV-PC (*E*), 10 μg/ml 9-HODE (*F*) or 10 μg/ml 13-HODE (*G*). *A* - *G*, representative donor analysis of CXCL16 surface expression on $CD36^+$ (top), $SR\text{-}A^+$ (center) or $CD68^+$ (bottom) cells at the indicated times. Treatments and incubation times are indicated at the top, isotype controls and mAbs used for flow cytometry are indicated on the left or bottom of FACS plots respectively. Numbers in the upper right corner of each quadrant indicate percent of total cells with the indicated immunophenotype. Representative donor was one of 8 tested in Figure 1. m IgMκ, mouse IgMκ; m IgG_1, mouse IgG_1; m IgG2bκ, mouse IgG2bκ.

Suppl. Figure 3. OxLDL, 9-HODE and 13-HODE downregulate ADAM10 surface expression on $CXCL16^+$ Mϕ. Representative population analysis of ADAM10 surface expression. Mo were incubated for 6, 12 or 24 h without or with 50 μg/ml LDL or 50 μg/ml oxLDL or alternatively with 10 μg/ml of each of the following lipids: PGPC, POV-PC, 9-HODE or 13-HODE. Stimulations and treatment times are indicated at the top of FACS plots. Numbers in the top right corner of each quadrant indicate percent of total cells with the

indicated immunophenotype. Representative donor was one of 3 tested in Figure 3. m IgG2bκ, mouse IgG2bκ.

Suppl. Figure 4. OxLDL and oxidized linoleic acid components of LDL upregulate CXCR6 on CASMCs. Analysis of CXCR6 surface expression on CASMCs. Cells were either cultured without lipids or were stimulated for 24 h with oxLDL (25 μg/ml), 9-HODE (5 μg/ml) or 13-HODE (5 μg/ml). Representative donor (top) analysis of CXCR6 surface expression (center) and summary data (bottom) which are presented as the mean ± SEM of the percent of $CXCR6^+$ cells. Treatments are indicated at the top of each FACS plot. Blue curve, isotype control mouse IgG2b.

Suppl. Figure 5. Optimization of sRNAi-mediated knockdown of endogenously expressed CXCL16 in Mo. Mo were cultured untransfected or transfected with the indicated concentrations of negative control ($-C_{med}$) or CXCL16-specific (CXCL16) sRNAi duplexes for 24 h with or without 50 μg/ml oxLDL, and CXCL16 surface and mRNA expression was monitored. *A,* Representative donor. Numbers in the top quadrant indicate the percent of $CXCL16^+$ cells. *B,* Summary data of the percent of total cells with the indicated immunophenotype. *C,* RNA analysis by real-time PCR. Results in *B* and *C* are shown as the mean ± SEM from 3 independent experiments using 3 different donors each condition tested in triplicate.

Suppl. Figure 6. oxLDL interferes with CXCL16-promoted Dil-HDL uptake in Mϕ. Mo were cultured with or without 50 μg/ml LDL or oxLDL for 24 h and incubated for 2 h at 37°C with 5 μg/ml Dil-HDL in the presence of access amounts of unlabeled LDL, HDL or oxLDL. Cell-associated Dil was measured at 520 nm/564 nm and expressed as nanograms of

Dil-HDL per milligram of total cellular protein. *A,* Cells were not treated with blocking agents prior to Dil-HDL internalization. *B,* Cells were incubated with either 4 μg/ml rat IgG2a or the equivalent amount of CXCL16 mAb before the assay. Results are from 4 independent experiments using 4 different donors each condition tested in duplicate. Data are expressed as the mean ± SEM.

A

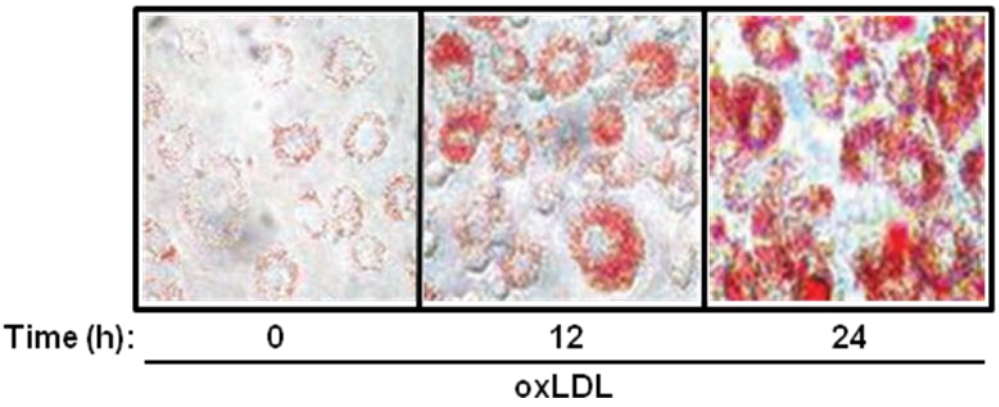

B

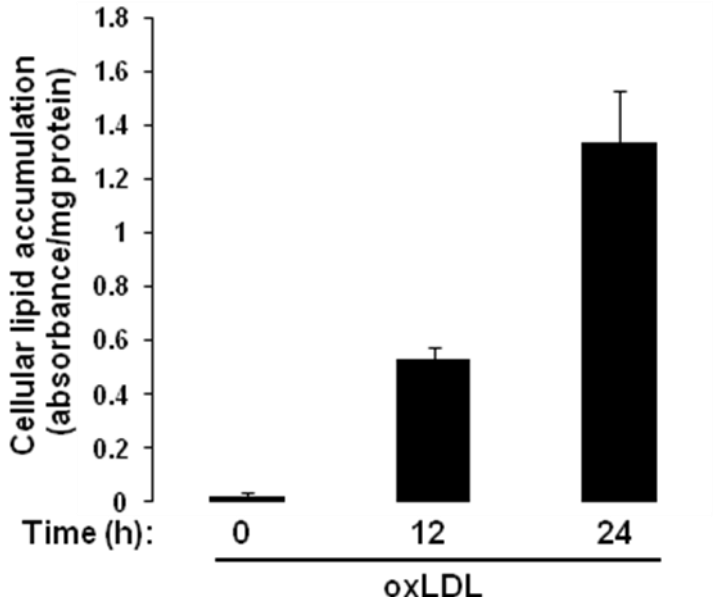

Barlic et al., Suppl. Figure 1

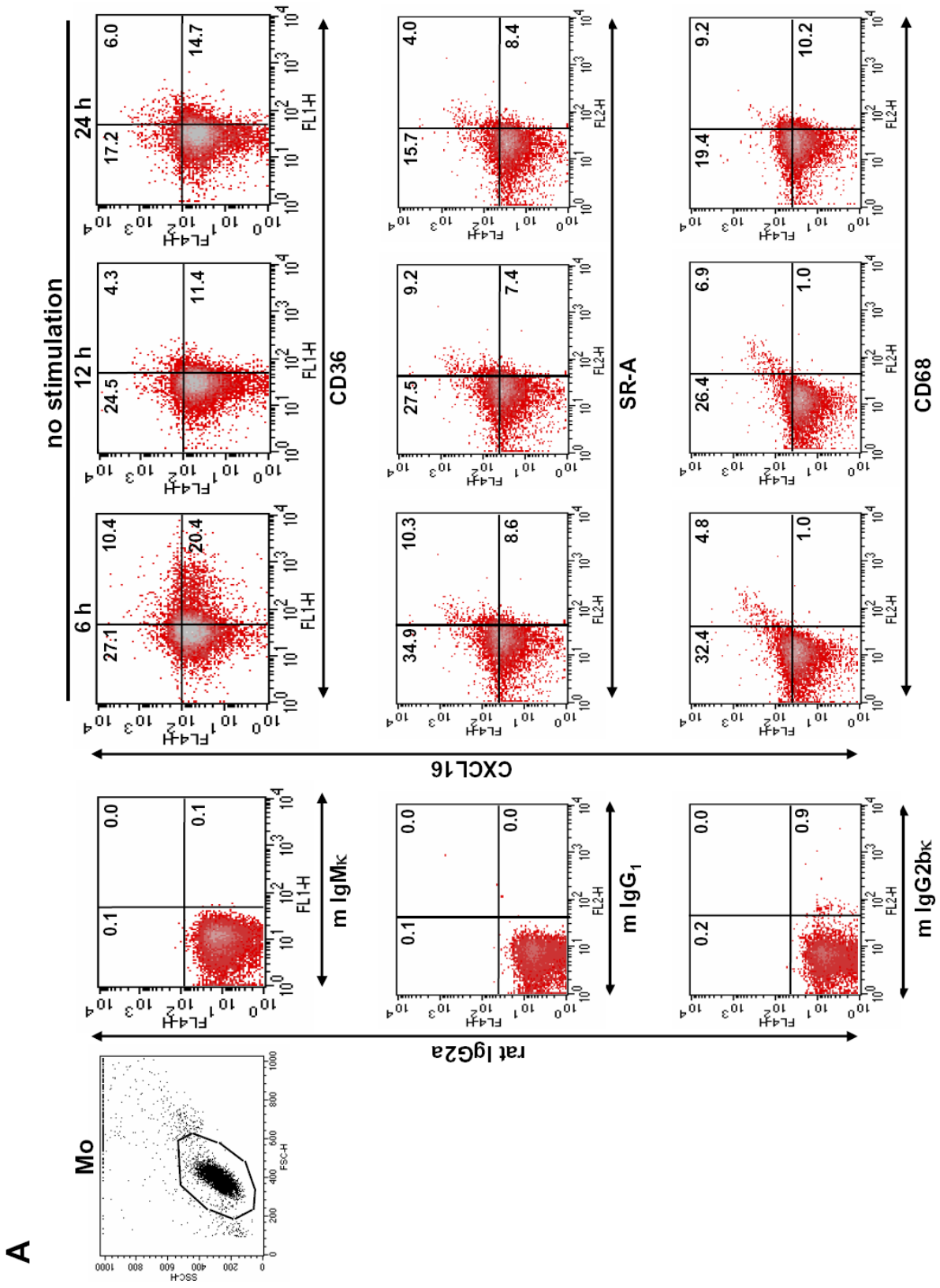

Barlic et al., Suppl. Figure 2

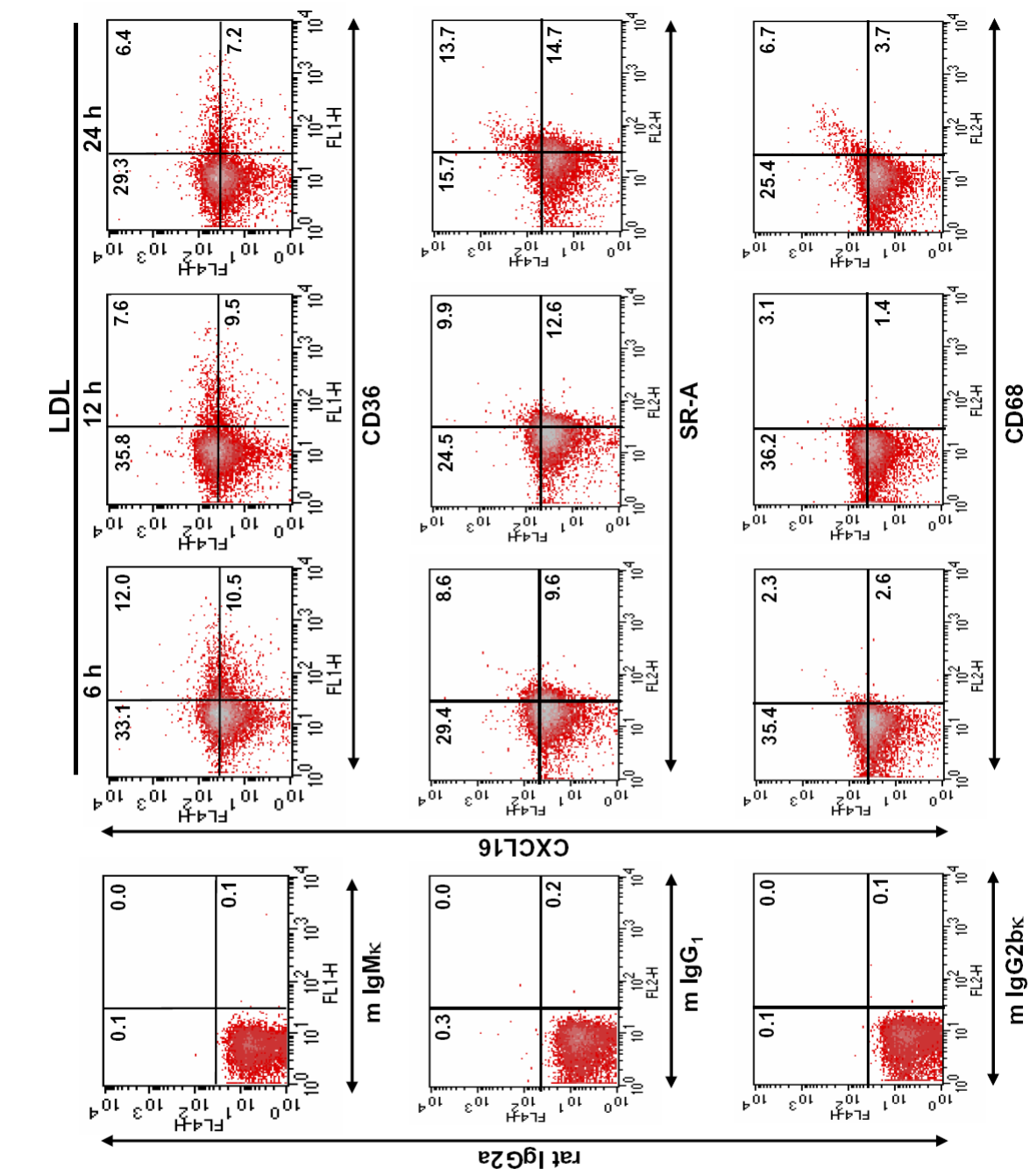

Barlic et al., Suppl. Figure 2

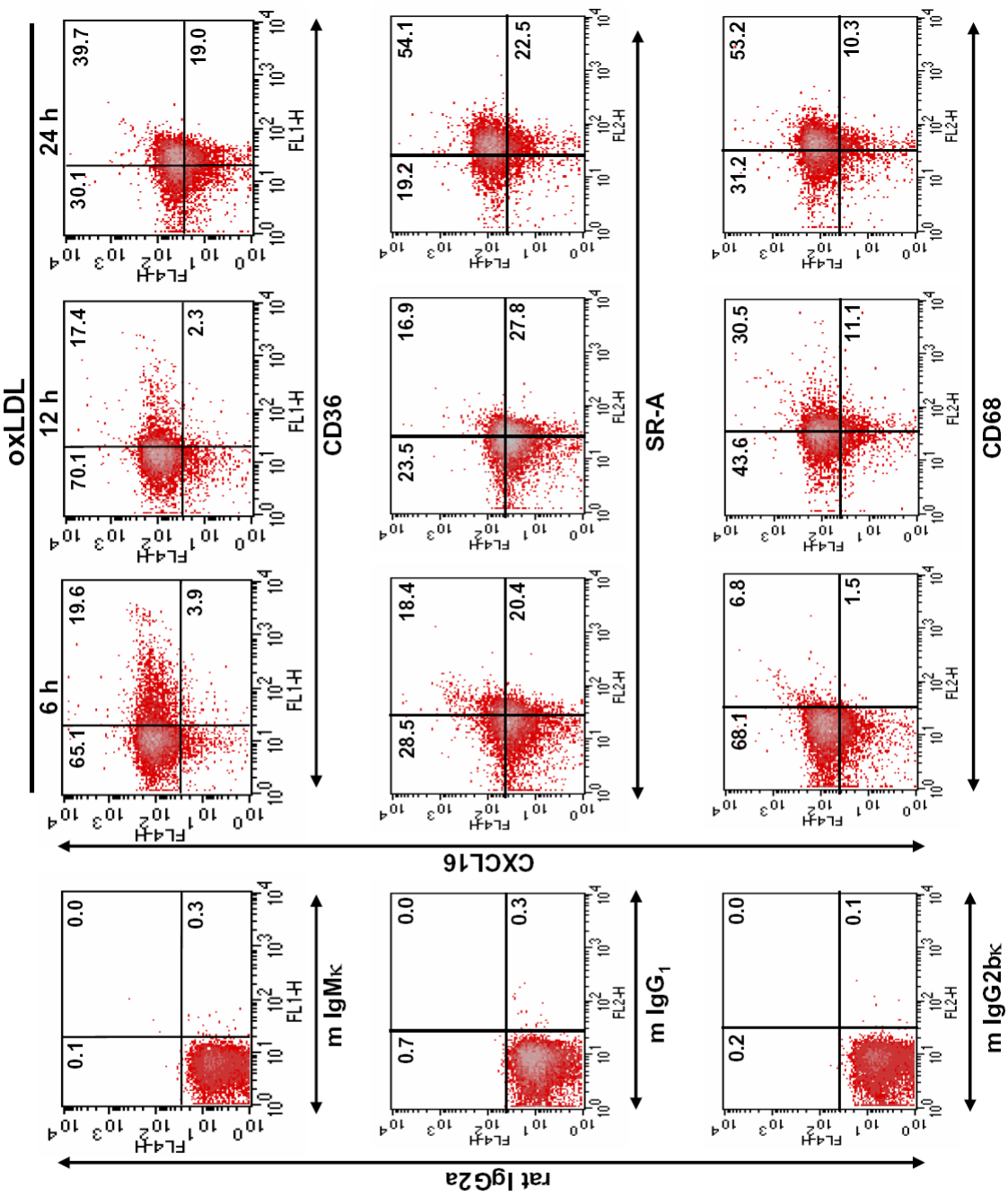

C

Barlic et al., Suppl. Figure 2

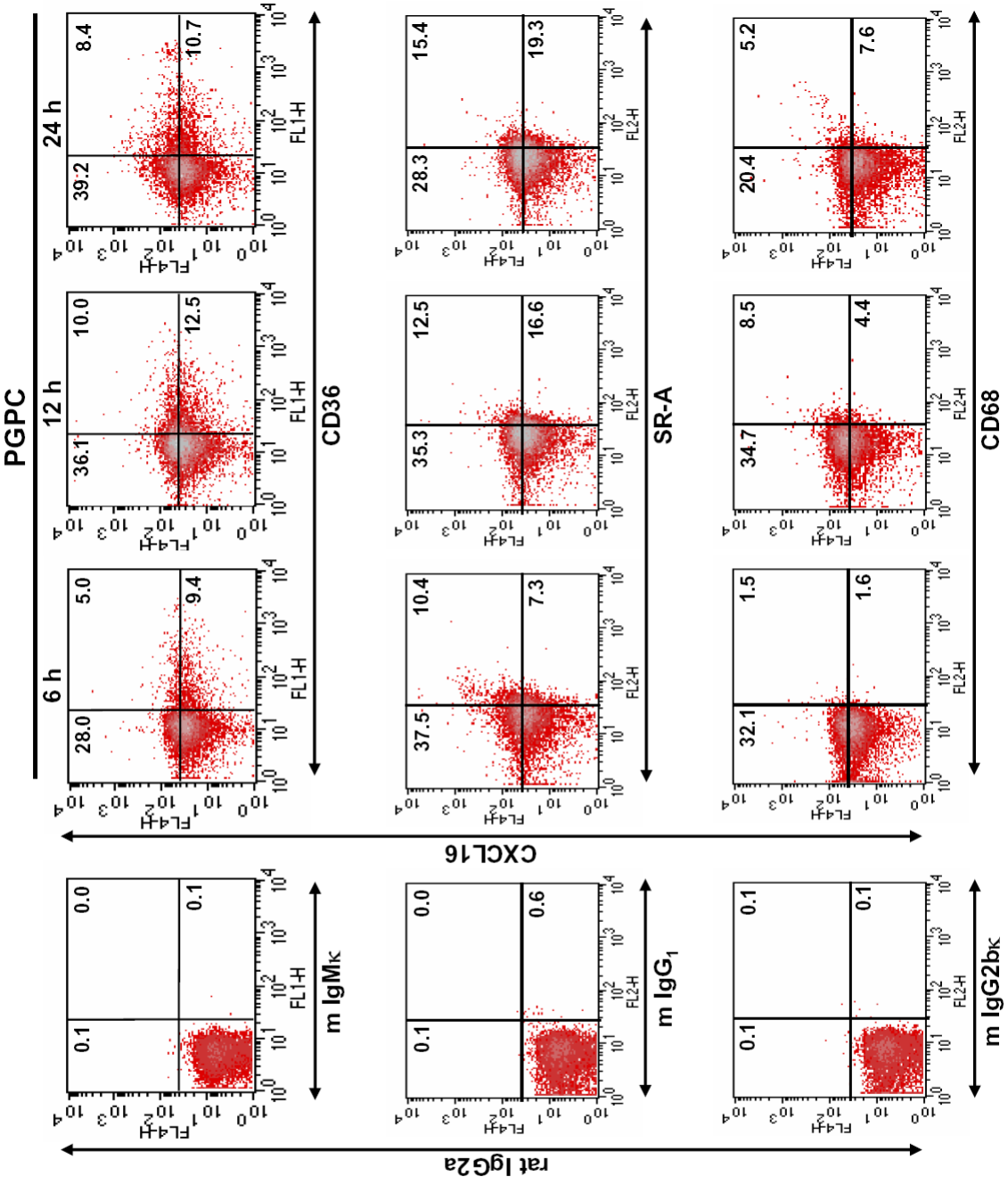

D

Barlic et al., Suppl. Figure 2

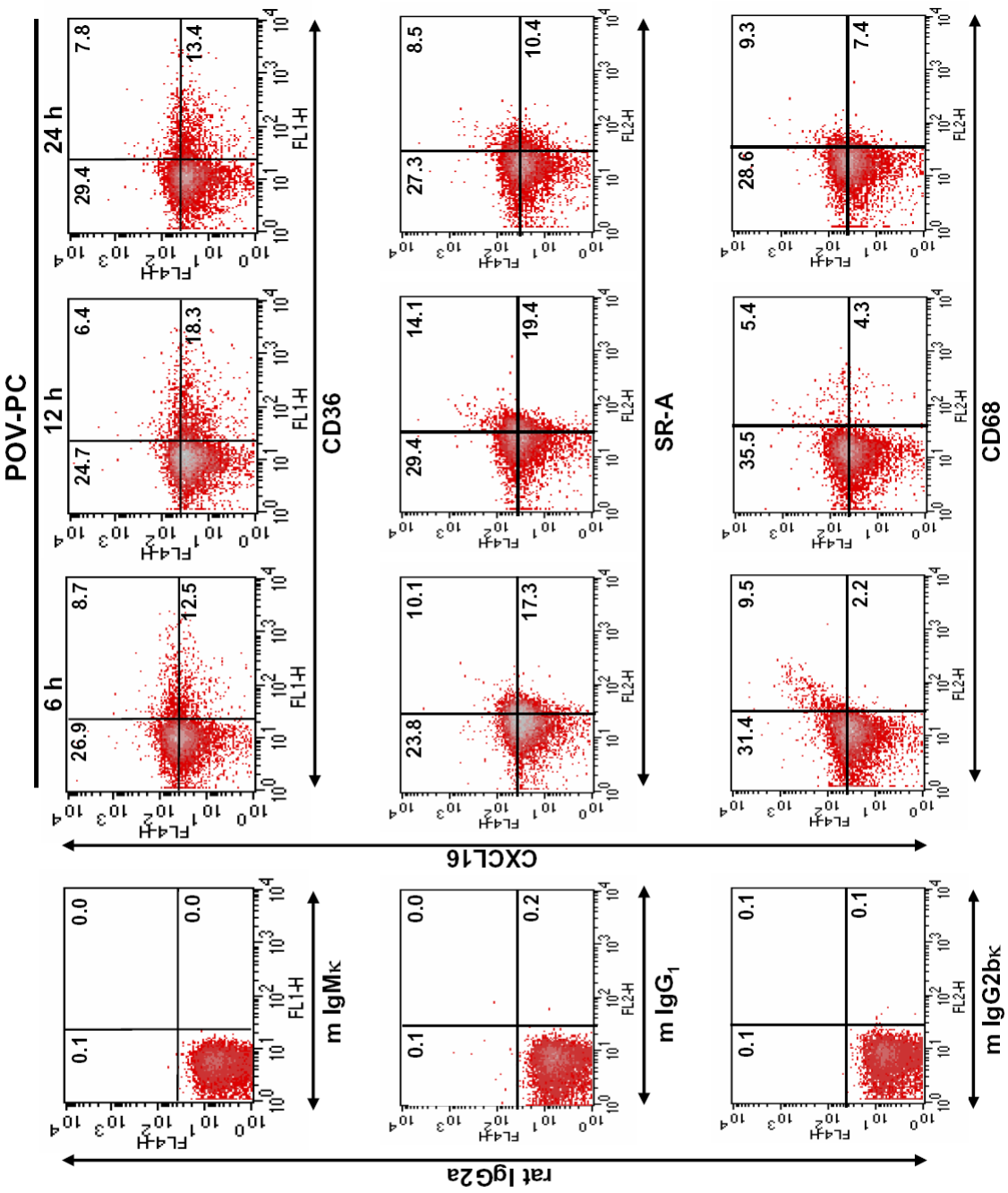

E

Barlic et al., Suppl. Figure 2

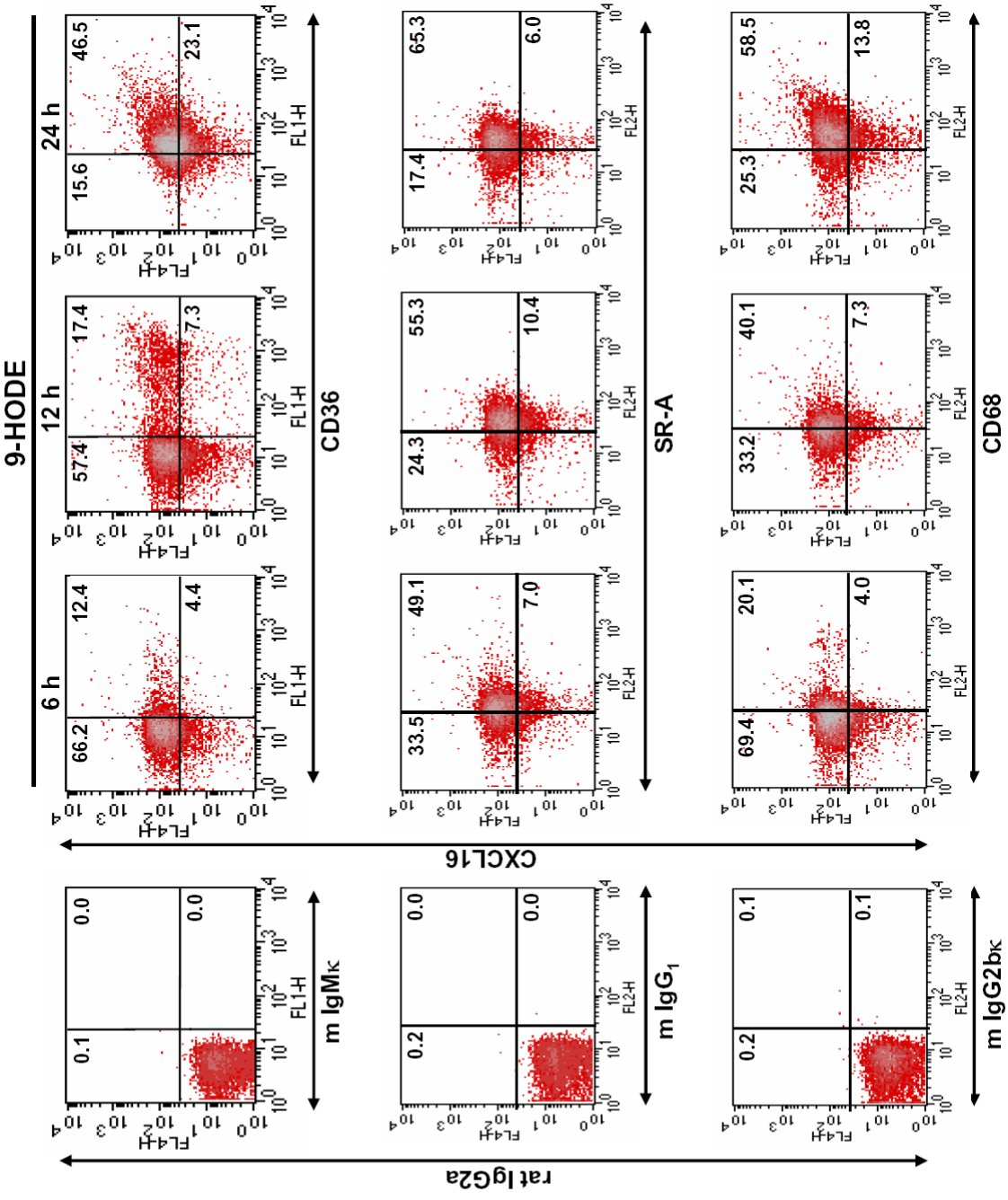

F

Barlic et al., Suppl. Figure 2

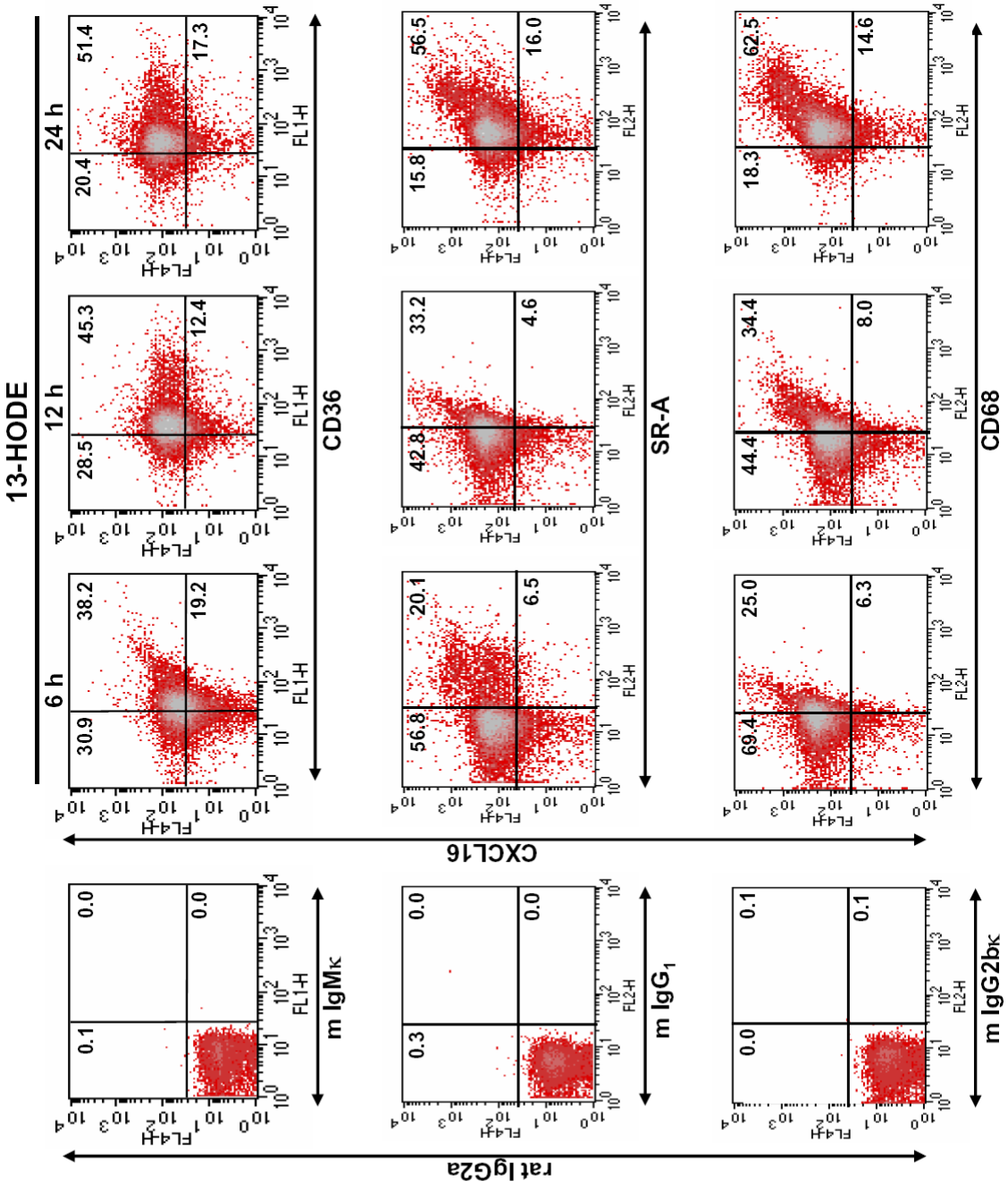

G

Barlic et al., Suppl. Figure 2

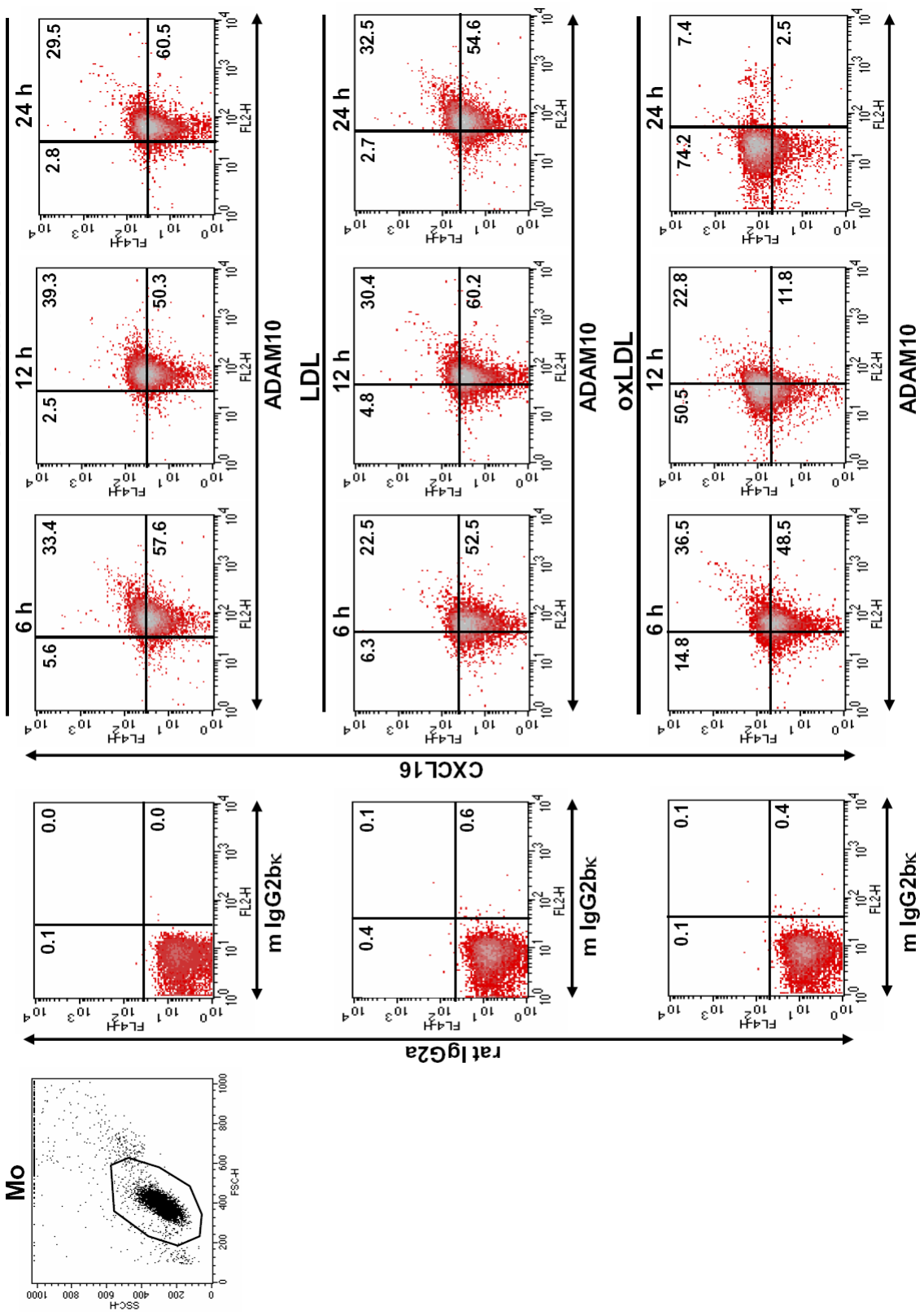

Barlic et al., Suppl. Figure 3

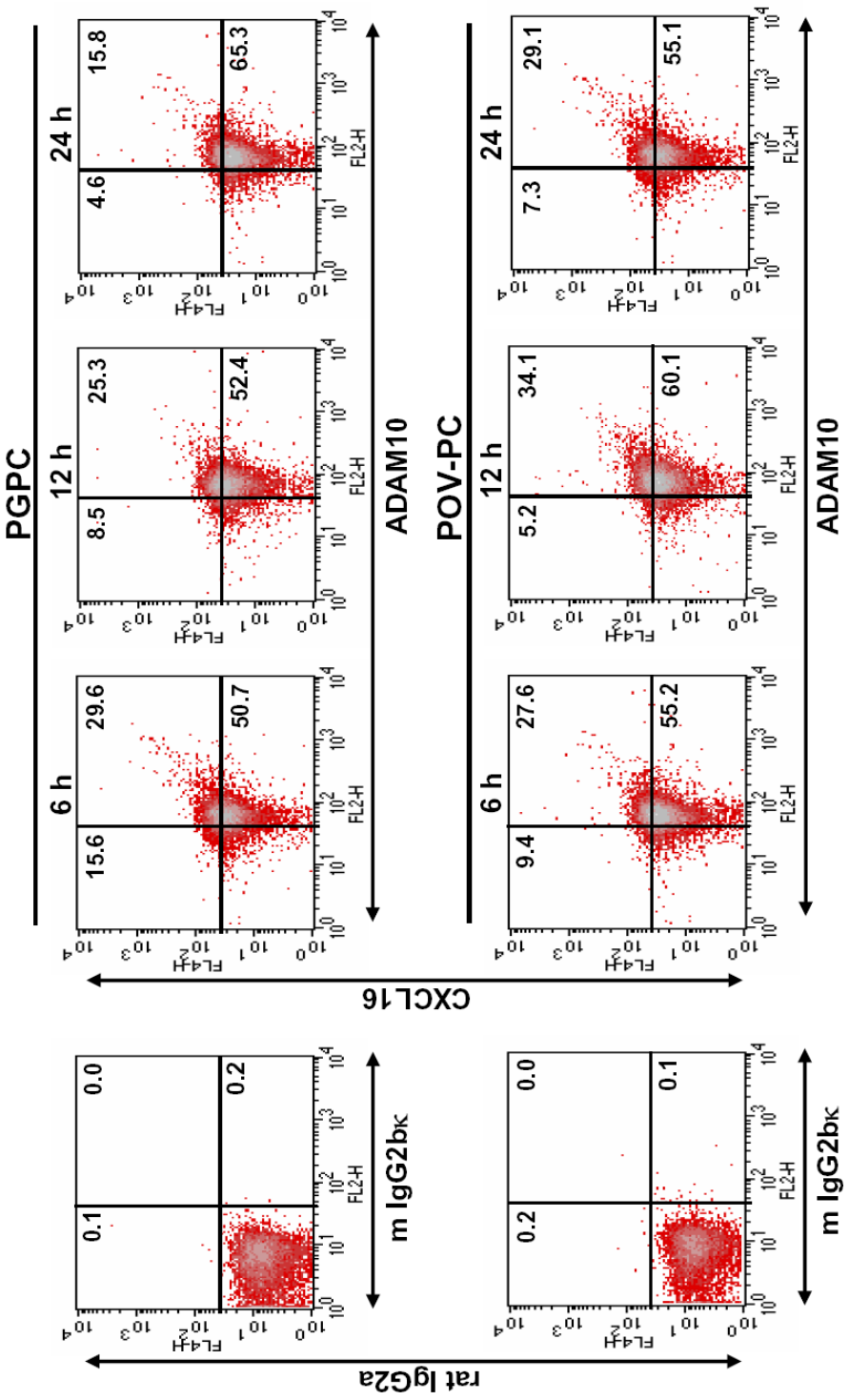

Barlic et al., Suppl. Figure 3

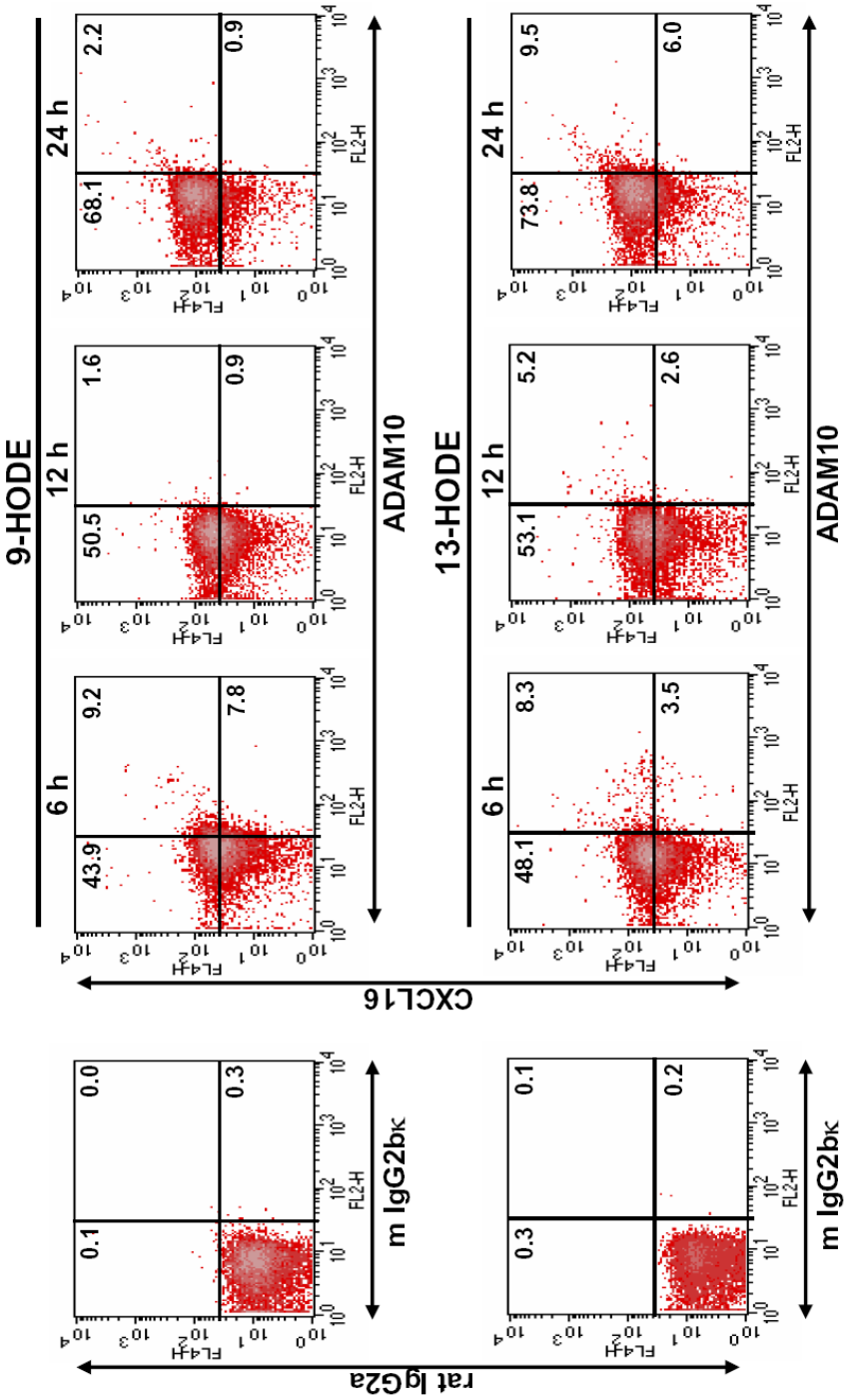

Barlic et al., Suppl. Figure 3

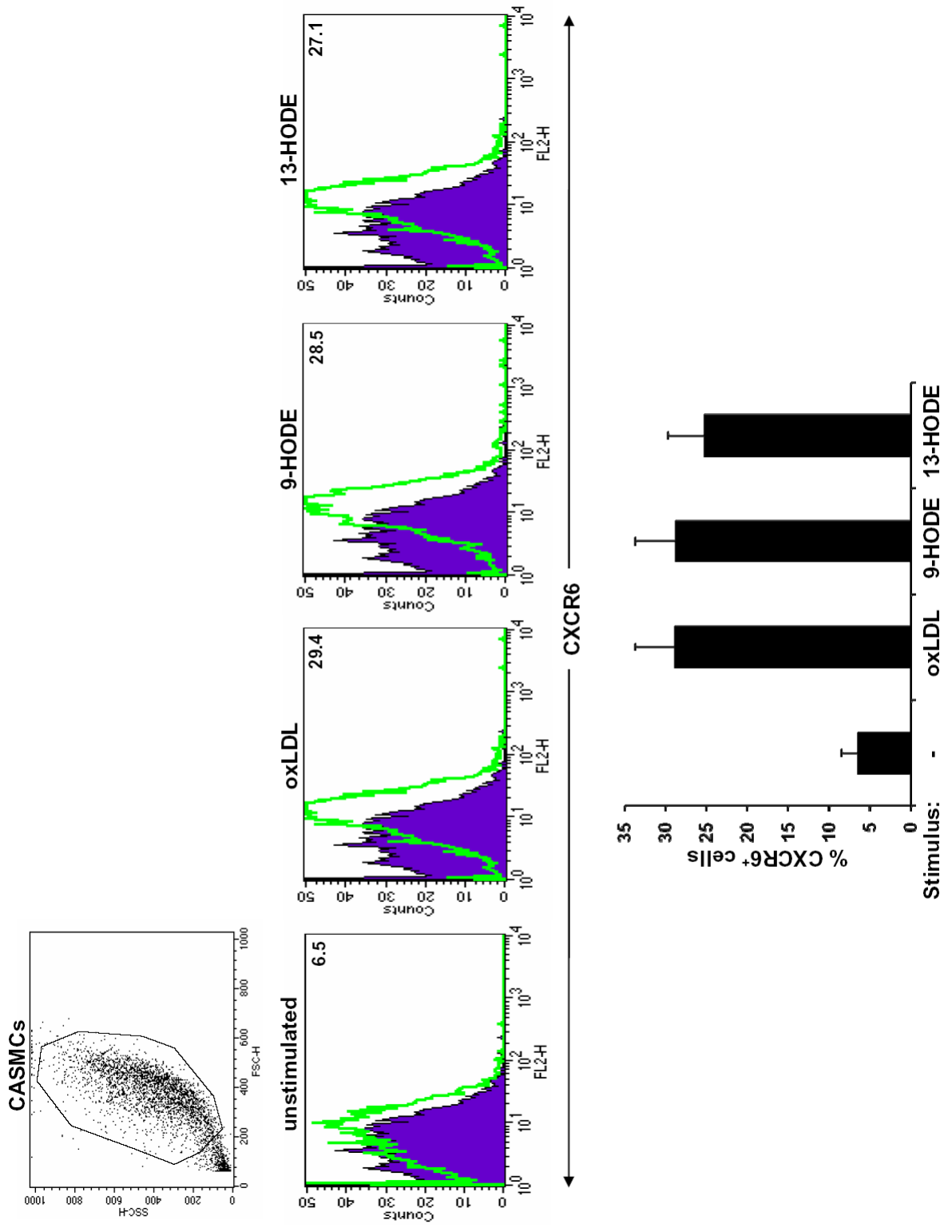

Barlic et al., Suppl. Figure 4

A

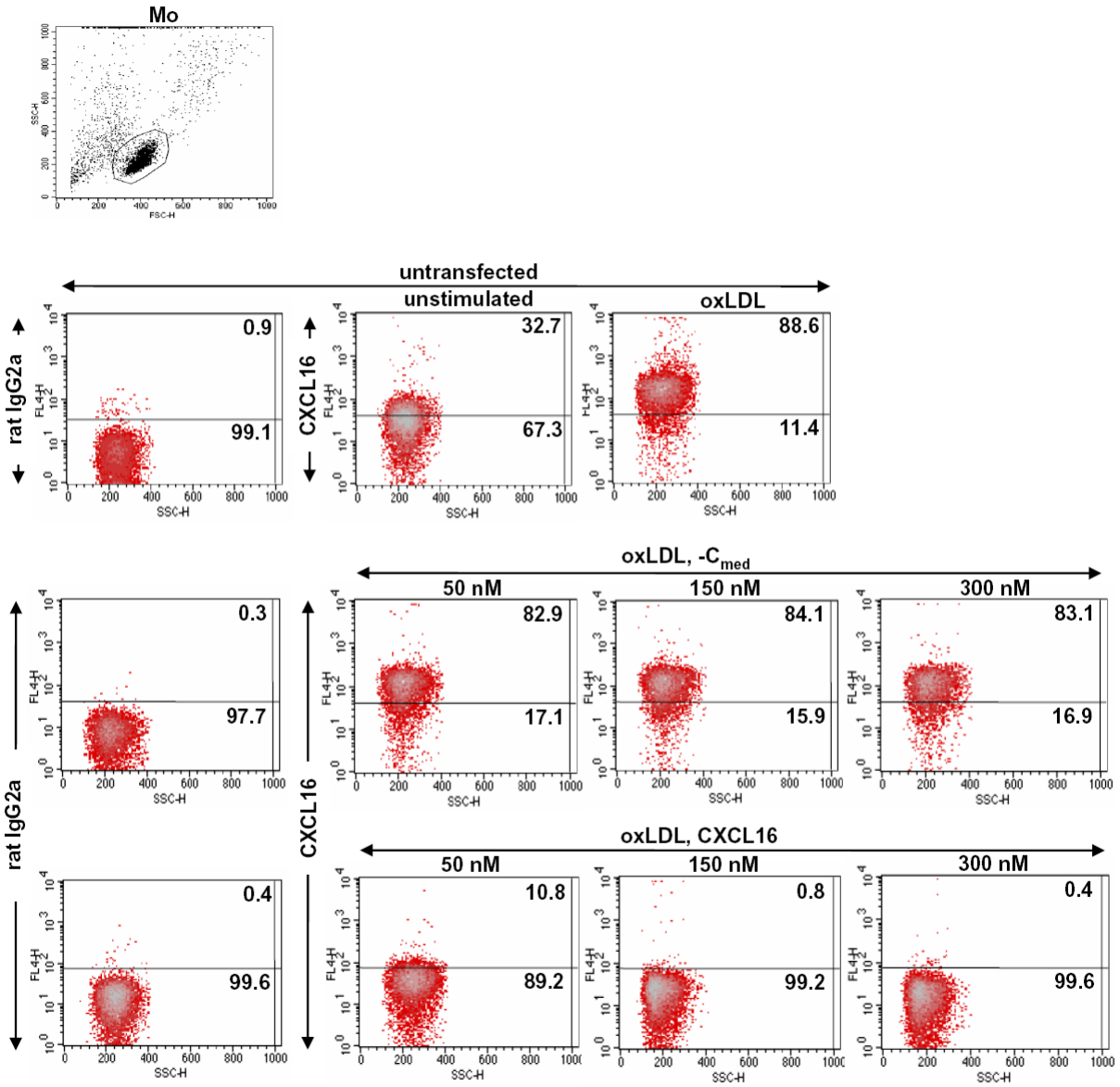

Barlic et al., Suppl. Figure 5

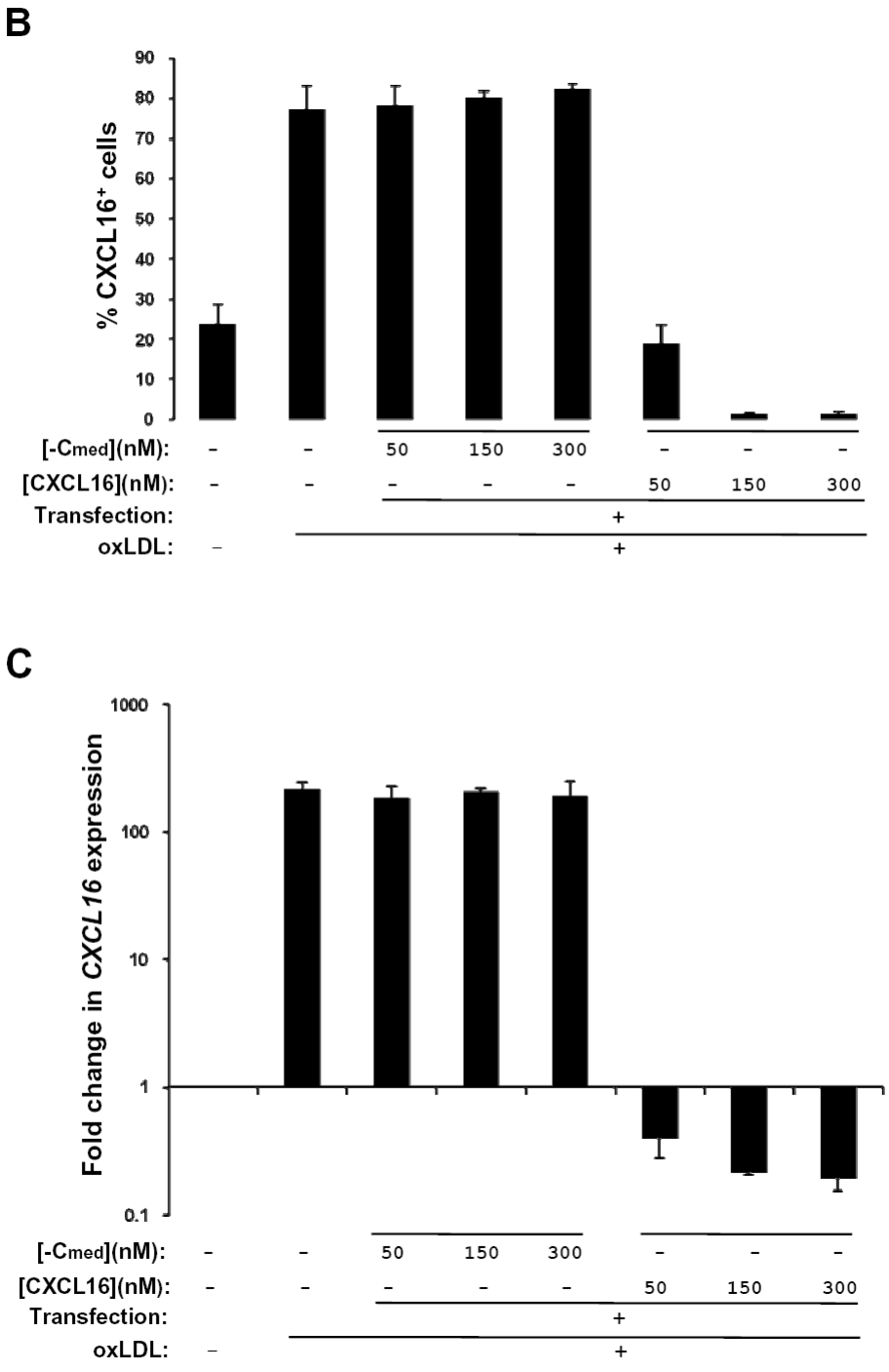

Barlic et al., Suppl. Figure 5

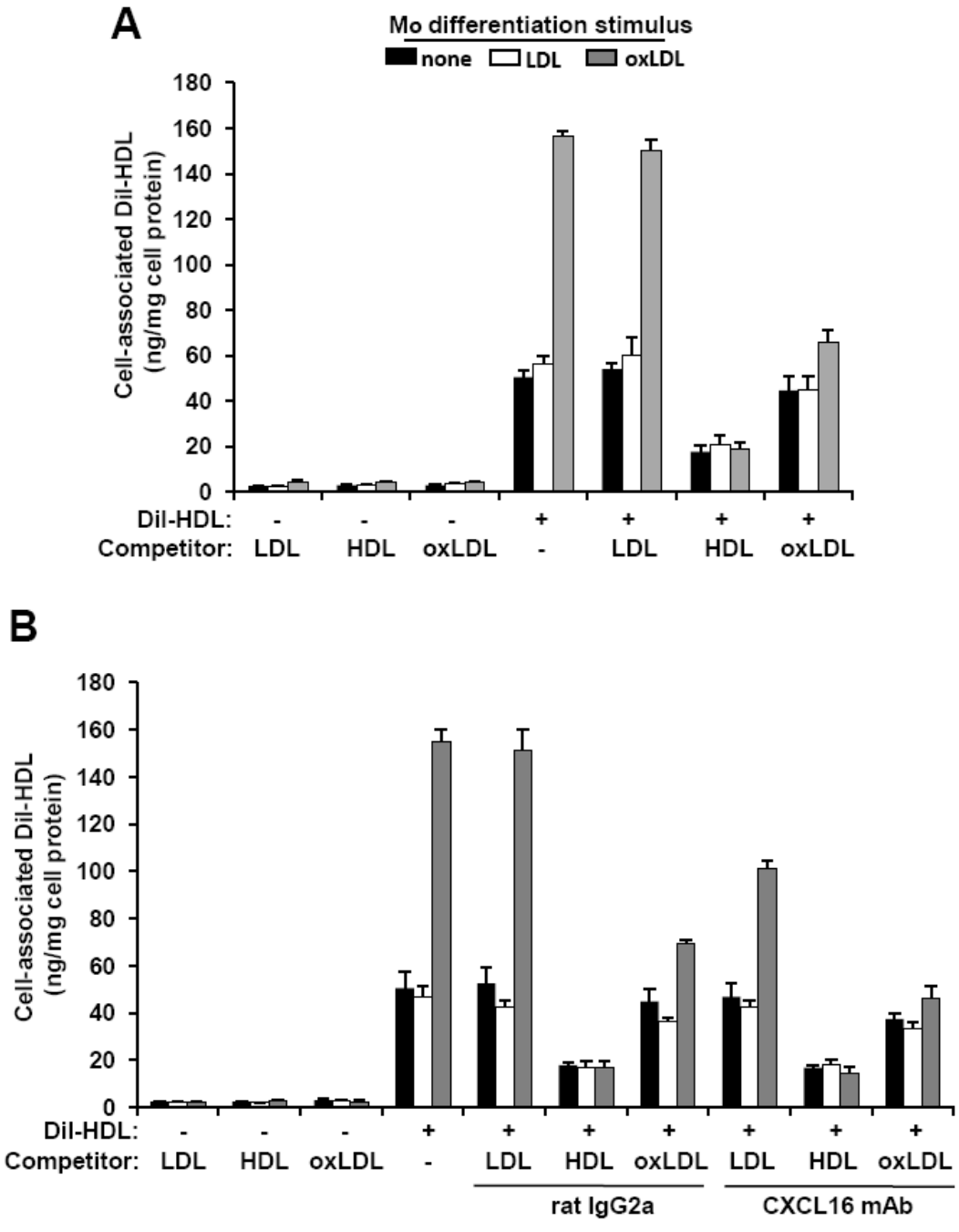

Barlic et al., Suppl. Figure 6